XIV International Conference on Computational Plasticity. Fundamentals and Applications
COMPLAS XIV
E. Oñate, D.R.J. Owen, D. Peric & M. Chiumenti (Eds)

CLOSED FORM SOLUTION OF THE RETURN MAPPING ALGORITHM IN ELASTOPLASTICITY

FABIO DE ANGELIS*, ROBERT L. TAYLOR†

* Department of Structures for Engineering and Architecture
University of Naples Federico II
Via Claudio 21, 80125 Naples, Italy
e-mail: fabio.deangelis@unina.it

†Department of Civil and Environmental Engineering
University of California, Berkeley
714 Davis Hall, Berkeley, CA 94720-1710, USA
e-mail: rlt@ce.berkeley.edu

Key words: Exact Closed Form Solution, Return Mapping Algorithm, Computational ElastoPlasticity.

Abstract. In the present work a return mapping algorithm is discussed for small strain elastoplasticity boundary value problems with an exact closed form solution of the local constitutive equations. Nonlinear kinematic hardening rules are adopted in modelling kinematic hardening behavior of ductile materials. The local solution of the constitutive equations is expressed by only one nonlinear scalar equation which is subsequently reduced to a single variable algebraic equation. Due to the straightforward form of the nonlinear scalar equation the analytical solution of the algebraic equation is found in exact closed form. A remarkable advantage of the present approach is that no iterative solution method is used to solve the local constitutive equations in three-dimensional elastoplasticity. Numerical applications and computational results are reported in order to illustrate the robustness and effectiveness of the proposed algorithmic procedure.

1 INTRODUCTION

In the present work a return mapping algorithm is discussed for small strain elastoplasticity boundary value problems with an exact closed form solution of the local constitutive equations, see De Angelis and Taylor [1]. Nonlinear kinematic hardening rules are adopted in modelling kinematic hardening behavior of ductile materials, see e.g. Armstrong and Frederick [2]. In fact, saturation hardening rules of the exponential type do not properly represent nonlinear kinematic hardening behavior since upon unloading and reloading the simulation does not suitably reproduce the material behavior in which it is exhibited renewed plasticity prior to the state at which unloading occurred.

One of the advantages of the present algorithmic procedure is to reduce the local solution of the constitutive equations to only one nonlinear scalar equation. In the literature other proposals have been presented which reduce the local constitutive equations to one nonlinear scalar equation. However in the present work a particularly simple form of nonlinear scalar equation is derived. In fact, herein the local constitutive equations are reduced to a single variable algebraic (polynomial) equation. Moreover, in the present approach due to the straightforward form of the nonlinear scalar equation the analytical solution of the algebraic equation is found in exact closed form. Accordingly, a remarkable advantage of the present approach is that no iterative solution method is used to solve the local constitutive equations in three-dimensional elastoplasticity.

The consistent tangent operator associated to the proposed formulation is derived for elastoplasticity models, thus ensuring a quadratic rate of asymptotic convergence when used with the Newton Raphson iterative method for the global solution procedure of the structural problem, see e.g. Zienkiewicz Taylor and Fox [3] and Simo and Hughes [4].

Numerical applications and computational results for cyclic loading conditions are finally reported in order to illustrate the robustness and effectiveness of the proposed algorithmic scheme. Accordingly, the robustness and effectiveness of the proposed computational procedure is illustrated with specific numerical examples.

2 THE CONTINUUM MODEL

We assume the body $\mathcal{B}$ in the reference configuration $\Omega \subset \Re^n$, with $1 \leq n \leq 3$, and we denote with $\mathcal{T} \subset \Re_+$ the time interval of interest and with $\boldsymbol{V}$ the space of displacements, $\boldsymbol{D}$ the strain space and $\boldsymbol{S}$ the dual stress space. Let us also indicate with $\mathbf{u} : \Omega \times \mathcal{T} \to \boldsymbol{V}$ the displacement and with $\boldsymbol{\sigma} : \Omega \times \mathcal{T} \to \boldsymbol{S}$ the stress tensor. The compatible strain tensor is defined as $\boldsymbol{\varepsilon} = \nabla^s \mathbf{u} : \Omega \times \mathcal{T} \to \boldsymbol{D}$, where ∇^s is the symmetric part of the gradient operator. We consider the stress tensor as additively decomposed into a deviatoric and a spherical part so that $\boldsymbol{\sigma} = \mathbf{s} + p\,\mathbf{1}$, where $\mathbf{s} \stackrel{\text{def}}{=} \text{dev}\boldsymbol{\sigma} = \boldsymbol{\sigma} - p\,\mathbf{1}$ is the stress deviator, $p \stackrel{\text{def}}{=} \frac{1}{3} tr(\boldsymbol{\sigma})$ is the pressure of the spherical part $p\,\mathbf{1}$ and $\mathbf{1}$ is the rank two identity tensor. The strain tensor is similarly decomposed into the deviatoric and volumetric parts $\boldsymbol{\varepsilon} = \mathbf{e} + \frac{1}{3}\theta\,\mathbf{1}$, where $\mathbf{e} \stackrel{\text{def}}{=} \text{dev}\boldsymbol{\varepsilon} = \boldsymbol{\varepsilon} - \frac{1}{3}\theta\,\mathbf{1}$ is the strain deviator and $\theta \stackrel{\text{def}}{=} tr(\boldsymbol{\varepsilon})$ is the change in volume. The relation between the spherical part of the stress and the volumetric part of the strain is described by $p = K\,\theta$, where K is the bulk modulus.

The linear elastic relation between the stress deviator and the elastic deviatoric strain is expressed by

$$\mathbf{s} = 2G\,\mathbf{e}^e = 2G[\mathbf{e} - \mathbf{e}^p], \tag{1}$$

in which G is the shear modulus, and the deviatoric part of the total strain has been additively decomposed into an elastic and a plastic part $\mathbf{e} = \mathbf{e}^e + \mathbf{e}^p$. The relative stress $\boldsymbol{\Sigma}$ is also expressed by

$$\boldsymbol{\Sigma} = \mathbf{s} - \boldsymbol{\alpha}, \tag{2}$$

where $\boldsymbol{\alpha}$ represents the deviatoric back stress.

A J_2 material behavior is assumed herein. Accordingly, a von Mises yield criterion is

adopted in the form

$$f(\boldsymbol{\sigma}, \boldsymbol{\alpha}, \kappa) = \|\mathrm{dev}\boldsymbol{\sigma} - \boldsymbol{\alpha}\| - \kappa(\chi_{iso}) = \|\mathbf{s} - \boldsymbol{\alpha}\| - \sqrt{\tfrac{2}{3}}(\sigma_{yo} + \chi_{iso}) \leq 0, \tag{3}$$

where $\kappa(\chi_{iso}) = \sqrt{\frac{2}{3}}\,\sigma_y = \sqrt{\frac{2}{3}}(\sigma_{yo} + \chi_{iso})$ is the current radius of the yield surface in the deviatoric plane and σ_{yo} is the uniaxial yield stress of the virgin material. The static internal variable for isotropic hardening is specified by $\chi_{iso} = H_{iso}\overline{e}^p$, where H_{iso} is the isotropic hardening modulus and where we assumed $\chi_{iso} \stackrel{\text{def}}{=} R$, being R the increment of the yield stress with respect to the uniaxial yield stress of the virgin material and $\overline{e}^p$ representing the equivalent (accumulated) plastic strain $\overline{e}^p \stackrel{\text{def}}{=} \int_0^t \sqrt{\frac{2}{3}}\|\dot{\mathbf{e}}^p\|\,\mathrm{d}\,t$. For a finer representation of the isotropic hardening it is often assumed

$$\chi_{iso} = H_{iso}(\overline{e}^p)^m, \qquad \text{or} \qquad R = R_\infty(1 - \mathrm{e}^{-b\,\overline{e}^p}), \tag{4}$$

where m, R_∞ and b are material parameters.

The evolutive flow law for the deviatoric plastic strain rate is expressed by

$$\dot{\mathbf{e}}^p = \dot{\gamma}\,\frac{\partial f}{\partial \boldsymbol{\sigma}} = \dot{\gamma}\,\frac{\partial f}{\partial \boldsymbol{\Sigma}} = \dot{\gamma}\,\mathbf{n}, \tag{5}$$

where $\dot{\gamma}$ is the plastic rate multiplier and $\mathbf{n} \stackrel{\text{def}}{=} \dfrac{\boldsymbol{\Sigma}}{\|\boldsymbol{\Sigma}\|}$ is the normal to the yield surface. Consequently, the equivalent plastic strain rate is supplied by $\dot{\overline{e}}^p = \sqrt{\frac{2}{3}}\,\dot{\gamma}$.

The rate of the back stress can be expressed by the Prager law [5]

$$\dot{\boldsymbol{\alpha}} = \tfrac{2}{3}\,H_{kin}\,\dot{\mathbf{e}}^p, \tag{6}$$

where H_{kin} is the kinematic hardening modulus. For a nonlinear kinematic hardening behavior it is often adopted the model proposed by Armstrong and Frederick [2]

$$\dot{\boldsymbol{\alpha}} = \tfrac{2}{3}\,H_{kin}\,\dot{\mathbf{e}}^p - H_{nl}\,\dot{\overline{e}}^p\,\boldsymbol{\alpha}, \tag{7}$$

where H_{nl} is a non-dimensional material dependent parameter. The second term of equation (7) is a recall term and $H_{nl} = 0$ stands for a linear kinematic hardening behavior. For a better approximation several models can be added with different recall constants (see e.g. [6])

$$\boldsymbol{\alpha} = \sum_{i=1}^{M} \boldsymbol{\alpha}_i, \qquad\qquad \dot{\boldsymbol{\alpha}}_i = \tfrac{2}{3}\,H_{kin,i}\,\dot{\mathbf{e}}^p - H_{nl,i}\,\dot{\overline{e}}^p\,\boldsymbol{\alpha}_i. \tag{8}$$

The Kuhn-Tucker optimality conditions

$$\dot{\gamma} \geq 0, \qquad f(\boldsymbol{\sigma}, \boldsymbol{\alpha}, \kappa) \leq 0, \qquad \dot{\gamma} f(\boldsymbol{\sigma}, \boldsymbol{\alpha}, \kappa) = 0, \tag{9}$$

represent the loading-unloading conditions and they complete the evolutive model in plasticity, see e.g. [3] and [4].

3 Algorithmic formulation

In the finite element formulation we adopt a *strain driven* approach. Accordingly, by knowing the strain and the solution at time t_n, represented by the set $(\mathbf{s}_n, \mathbf{e}_n, \mathbf{e}^p_n, \overline{e}^p_n, \boldsymbol{\alpha}_n)$, we need to determine the solution at time t_{n+1} represented by the set $(\mathbf{s}, \mathbf{e}, \mathbf{e}^p, \overline{e}^p, \boldsymbol{\alpha})$. By adopting a backward Euler integration scheme, the evolutive equation for the deviatoric plastic strain rate (5) and the equivalent plastic strain rate are given respectively by

$$\mathbf{e}^p = \mathbf{e}^p_n + \lambda\,\mathbf{n}, \qquad\qquad \overline{e}^p = \overline{e}^p_n + \sqrt{\tfrac{2}{3}}\,\lambda, \tag{10}$$

where we have set $\lambda \stackrel{\text{def}}{=} \Delta\gamma_{n+1} = \dot{\gamma}_{n+1}\Delta t$.

The discrete form of the evolution law for the back stress is given by

$$\boldsymbol{\alpha} - \boldsymbol{\alpha}_n = \tfrac{2}{3}\,H_{kin}\lambda\mathbf{n} - H_{nl}\sqrt{\tfrac{2}{3}}\lambda\boldsymbol{\alpha}, \tag{11}$$

which can be expressed as

$$\boldsymbol{\alpha} = T^\lambda\boldsymbol{\alpha}_n + \tfrac{2}{3}\,H_{kin}T^\lambda\lambda\mathbf{n}, \tag{12}$$

where we have set

$$R^\lambda = (1 + \sqrt{\tfrac{2}{3}}\,H_{nl}\lambda), \qquad\qquad T^\lambda = \frac{1}{R^\lambda} = \frac{1}{(1 + \sqrt{\frac{2}{3}}\,H_{nl}\lambda)}. \tag{13}$$

In the above expressions we have adopted the superscript λ to denote a dependence on the increment of the plastic rate multiplier in the step $t_n \to t_{n+1}$.

Taking into account equation $(10)_1$ the deviatoric stress is given by

$$\mathbf{s} \;= 2G[\mathbf{e} - \mathbf{e}^p_n] - 2G\lambda\mathbf{n}, \tag{14}$$

and, by considering equation (12), the relative stress is expressed by

$$\boldsymbol{\Sigma} \;= \mathbf{s} - \boldsymbol{\alpha} = 2G[\mathbf{e} - \mathbf{e}^p_n] - T^\lambda\boldsymbol{\alpha}_n - U^\lambda\mathbf{n}, \tag{15}$$

where we have set

$$U^\lambda = [2G + \tfrac{2}{3}\frac{H_{kin}}{R^\lambda}]\lambda = [2G + \tfrac{2}{3}H_{kin}T^\lambda]\lambda. \tag{16}$$

An elastic predictor-plastic corrector scheme is adopted by means of a return mapping algorithm. By enforcing the satisfaction of the limit equations at time t_{n+1} the increment λ of the plastic rate parameter is computed. The variables are then updated according to the equations

$$\begin{cases} \mathbf{e}^p = \mathbf{e}^{p,TR} + \lambda\mathbf{n} \\ \overline{e}^p = \overline{e}^{p,TR} + \sqrt{\frac{2}{3}}\lambda \\ \boldsymbol{\alpha} = T^\lambda\boldsymbol{\alpha}^{TR} + \frac{2}{3}H_{kin}T^\lambda\lambda\mathbf{n} \\ \mathbf{s} \;= \mathbf{s}^{TR} - 2G\lambda\mathbf{n} \\ \boldsymbol{\Sigma} \;= \mathbf{s}^{TR} - T^\lambda\boldsymbol{\alpha}^{TR} - U^\lambda\mathbf{n}. \end{cases} \tag{17}$$

The relative stress $(17)_5$ is also expressed by

$$\boldsymbol{\Sigma} = \boldsymbol{\Sigma}^{TR} + (1 - T^{\lambda})\boldsymbol{\alpha}^{TR} - U^{\lambda}\mathbf{n}, \tag{18}$$

where $\boldsymbol{\Sigma}^{TR} \stackrel{\text{def}}{=} \mathbf{s}^{TR} - \boldsymbol{\alpha}^{TR}$ is the trial value of the relative stress typically adopted in plasticity with linear kinematic hardening.

In the proposed approach for plasticity with nonlinear kinematic hardening rules we find useful to introduce a trial-like value of the relative stress

$$\boldsymbol{\Sigma}^{\lambda}_{NLK} \stackrel{\text{def}}{=} \mathbf{s}^{TR} - T^{\lambda}\boldsymbol{\alpha}^{TR} \tag{19}$$

Accordingly, equation (18) can be expressed by

$$\boldsymbol{\Sigma} = \boldsymbol{\Sigma}^{\lambda}_{NLK} - U^{\lambda}\mathbf{n}, \tag{20}$$

Herein, we emphasize that for plasticity with nonlinear kinematic hardening the trial-like value $\boldsymbol{\Sigma}^{\lambda}_{NLK}$ depends upon λ, whereas the conventional trial value $\boldsymbol{\Sigma}^{TR}$ adopted in plasticity with linear kinematic hardening is independent of λ. The second rank tensor $\mathbf{n}$ is expressed by

$$\mathbf{n} = \frac{\partial f}{\partial \boldsymbol{\sigma}} = \frac{\partial f}{\partial \boldsymbol{\Sigma}}\frac{\partial \boldsymbol{\Sigma}}{\partial \boldsymbol{\sigma}} = \frac{\partial f}{\partial \boldsymbol{\Sigma}}\frac{\partial(\mathrm{dev}\boldsymbol{\sigma} - \boldsymbol{\alpha})}{\partial \boldsymbol{\sigma}} = \frac{\partial \|\boldsymbol{\Sigma}\|}{\partial \boldsymbol{\Sigma}}\mathbf{I}_{dev} = \frac{\boldsymbol{\Sigma}}{\|\boldsymbol{\Sigma}\|}\mathbf{I}_{dev} = \frac{\boldsymbol{\Sigma}}{\|\boldsymbol{\Sigma}\|}, \tag{21}$$

where $\mathbf{I}_{dev} = \mathbf{I} - \frac{1}{3}(\mathbf{1}\otimes\mathbf{1})$. Given the expressions (19) and (20), the tensor $\mathbf{n}$ also depends upon λ. This is at variance with respect to plasticity with linear kinematic hardening, where $\mathbf{n}$ is independent from λ. Accordingly, the algorithmic procedure for plasticity with nonlinear kinematic hardening is more complex.

We note from equation (21) that $\boldsymbol{\Sigma}$ is collinear with $\mathbf{n}$. From equation (20) we also derive that $\boldsymbol{\Sigma}^{\lambda}_{NLK}$ must be collinear with $\mathbf{n}$, and therefore $\boldsymbol{\Sigma}^{\lambda}_{NLK} = \|\boldsymbol{\Sigma}^{\lambda}_{NLK}\|\mathbf{n}$. Accordingly, we observe that in plasticity with nonlinear kinematic hardening it results

$$\mathbf{n}(\lambda) = \frac{\boldsymbol{\Sigma}(\lambda)}{\|\boldsymbol{\Sigma}(\lambda)\|} = \frac{\boldsymbol{\Sigma}^{\lambda}_{NLK}(\lambda)}{\|\boldsymbol{\Sigma}^{\lambda}_{NLK}(\lambda)\|}. \tag{22}$$

Consequently, the present approach to plasticity with nonlinear kinematic hardening has the advantage that the equation (20) preserves a nonlinear scalar equation in λ

$$\|\boldsymbol{\Sigma}\| = \|\boldsymbol{\Sigma}^{\lambda}_{NLK}\| - U^{\lambda}. \tag{23}$$

As shown in the following section the above equation represents an algebraic (polynomial) equation in the single variable λ. Once the increment λ of the plastic rate parameter is determined the variables are updated at time t_{n+1} by considering equations (17) and taking into account equation (22).

4 Nonlinear scalar equation in λ

Equation (23) yields the novel expression of the nonlinear scalar equation which is solved for determining the increment λ of the plastic rate parameter. Accordingly, in the present approach the local solution of the constitutive equations reduces to only one nonlinear scalar equation. In the literature other proposals have been presented in which the constitutive equations are reduced to a nonlinear scalar equation, see e.g. Hartmann Luhrs and Haupt [7] and Kobayashi and Ohno [8]. With respect to such proposals, the present approach has the advantage that the constitutive equations are reduced to only one *single variable algebraic (quartic) equation* which is a particularly simple form of nonlinear scalar equation. Remarkably, in the present approach no numerical procedures are required to accelerate convergence for the solution of the nonlinear scalar equation, such as for instance the Aitken's process adopted in [8]. In fact, in the proposed formulation the search for the analytical solutions of the nonlinear scalar equation is pursued in exact closed form, i.e. with no recourse to iterative methods. This particular feature ensures efficiency and robustness to the overall computational procedure.

The limit function (3) is expressed as $\|\boldsymbol{\Sigma}\| - \sqrt{\frac{2}{3}}\sigma_y = 0$. Accordingly, the equation (23) supplies

$$\|\boldsymbol{\Sigma}^{\lambda}_{NLK}\| - U^{\lambda} - \sqrt{\tfrac{2}{3}}\sigma_y = 0, \tag{24}$$

and by setting

$$\begin{aligned} S_{ss} &= \mathbf{s}^{TR} \cdot \mathbf{s}^{TR} = \|\mathbf{s}^{TR}\|^2 \\ S_{s\alpha} &= \mathbf{s}^{TR} \cdot \boldsymbol{\alpha}^{TR} \\ S_{\alpha\alpha} &= \boldsymbol{\alpha}^{TR} \cdot \boldsymbol{\alpha}^{TR} = \|\boldsymbol{\alpha}^{TR}\|^2, \end{aligned} \tag{25}$$

after some algebra (see De Angelis and Taylor [1]) we obtain the quartic algebraic equation

$$g(\lambda) = C_1\lambda^4 + C_2\lambda^3 + C_3\lambda^2 + C_4\lambda + C_5 = 0, \tag{26}$$

where the coefficients of the quartic equation are given by De Angelis and Taylor [1]. For more details see De Angelis and Taylor [1] and De Angelis and Taylor [9] where a comprehensive treatment of the present approach is illustrated.

The present form of nonlinear scalar equation is at variance from the nonlinear scalar equation presented by Auricchio and Taylor [10] since it is generated by a different algorithmic scheme. Further, in [10] the solution of the nonlinerar scalar equation was performed by a Newton's iterative method, which for complex constitutive equations and highly nonlinear scalar equations sometimes experiences failures due to the occurring high gradients and the resulting round-off errors. One of the advantages of the present algorithmic scheme is that the local constitutive equations condense in a particularly simple form of nonlinear scalar equation, that is a *quartic algebraic equation*. Consequently, in the present approach the solutions of the quartic algebraic equation are determined in exact closed form, see among others Abramowitz [11], Beyer [12], and Hacke [13], and no iterative procedure is required to solve the local constitutive problem. Accordingly,

the increment λ of the plastic rate parameter in the step $t_n \to t_{n+1}$ is evaluated as the smallest positive real root of the quartic algebraic equation (26).

For more details see De Angelis and Taylor [1]. An alternative formulation resulting in a different algorithmic scheme associated to a different algorithmic form of the consistency condition and a different consistent tangent operator has also been presented by De Angelis and Taylor [9].

5 Consistent tangent operator

In the present section we illustrate the expression of the consistent tangent operator associated to the present algorithmic scheme which ensures a fast and robust numerical solution procedure for the iterative solution of the structural problem in elastoplasticity. The proposed numerical scheme ensures a quadratic rate of asymptotic convergence to the Newton Raphson iterative method for the solution of the global structural problem.

The linearization of the discrete forms of the evolutive equations for the stress deviator and the back stress yields a consistent tangent operator expressed by

$$\begin{aligned}\mathbf{D}_{discr} = \big\{ & K(\mathbf{1}\otimes\mathbf{1}) + [2G\ (1 - C^{NLK}_{discr})]\,\mathbf{I}_{dev} + [2G\,(C^{NLK}_{discr} - A^{NLK}_{discr}) \\ & + B^{NLK}_{discr}(\mathbf{n}\cdot\boldsymbol{\alpha})](\mathbf{n}\otimes\mathbf{n}) - B^{NLK}_{discr}(\boldsymbol{\alpha}\otimes\mathbf{n})\big\}\,,\end{aligned} \tag{27}$$

where we have set

$$\begin{aligned} a &= \frac{2G\,\lambda}{\|\boldsymbol{\Sigma}\|}, & b &= \tfrac{2}{3}\,\frac{H_{kin}\lambda}{\|\boldsymbol{\Sigma}\|}, \\ R^\lambda &= (1 + \sqrt{\tfrac{2}{3}}\,H_{nl}\lambda), & T^\lambda &= \frac{1}{R^\lambda}, & W^\lambda &= b + R^\lambda + aR^\lambda, \\ A^{NLK}_{discr} &= \frac{2G}{[2G + \frac{2}{3}H_{iso} + \frac{2}{3}H_{kin}T^\lambda - \sqrt{\frac{2}{3}}H_{nl}T^\lambda(\mathbf{n}\cdot\boldsymbol{\alpha})]}, \\ B^{NLK}_{discr} &= A^{NLK}_{discr}T^\lambda C^{NLK}_{discr}\sqrt{\tfrac{2}{3}}H_{nl}, & C^{NLK}_{discr} &= a\frac{R^\lambda}{W^\lambda}. \end{aligned} \tag{28}$$

The expression of the consistent tangent operator results to be non-symmetric due to the last term of equation (27), as is typically in elastoplasticity with nonlinear kinematic hardening rules. For more details on the development of the consistent tangent operator see De Angelis and Taylor [1].

For the derivation of the consistent tangent operator associated to the algorithmic procedure it is necessary to perform matrix inversions. At variance with respect to such usual approach, an alternative algorithmic formulation which is able to provide a consistent tangent operator without the necessity to perform matrix inversions has been presented by De Angelis and Taylor [9].

Other various algorithmic formulations have been presented e.g. by Nukala [14], Artioli Auricchio and Beirao da Veiga [15], De Angelis and Cancellara [16], De Angelis and Taylor [17], Artioli and Bisegna [18], Artioli Castellazzi and Krysl [19], Castellazzi Artioli and Krysl [20].

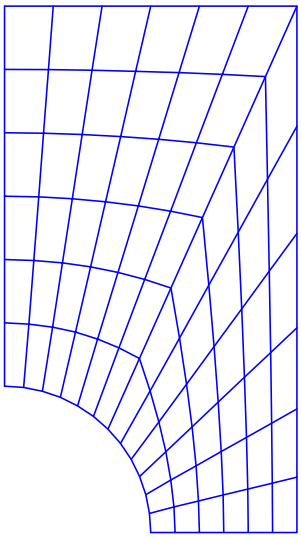

Figure 1: Perforated strip. Geometry and finite element mesh.

6 Computational results

The algorithmic formulation illustrated in the present work may be used for any 2-d or 3-d element which accepts a strain-driven approach. In our analysis we use 4-node quadrilateral elements with 2×2 Gaussian quadrature and the mixed approach described in Sec. 2.6.2 of Zienkiewicz Taylor and Fox [3]. The numerical scheme is implemented into the Finite Element Analysis Program (FEAP), see Zienkiewicz Taylor and Fox [3], and Taylor [21].

6.1 Numerical example: perforated strip

In the numerical example we consider the problem of an infinitely long rectangular strip with a circular hole in its axial direction, subject to increasing extension in a direction perpendicular to the axis of the strip and parallel to one of its sides. The geometry of the problem is illustrated in Fig. 1. For symmetry reasons only 1/4 of the strip needs to be considered. The dimensions of the rectangular section containing 1/4 of the strip are 18 mm for the long side and 10 mm for the short side. The radius of the circular hole is 5 mm. The adopted mesh consists of 91 nodes and 72 elements.

The mechanical properties of the material are: elastic modulus $E = 208000$ MPa, Poisson's ratio $\nu = 0.3$, yield limit $\sigma_{yo} = 170$ MPa, kinematic hardening modulus $H_{kin} = 41080$ MPa, nonlinear kinematic hardening parameter $H_{nl} = 525$, isotropic hardening modulus $H_{iso} = 2100$ MPa. The prescribed displacement at the top boundary is $u_o = 0.0025$ mm. The evolution with time of the proportional load coefficient $p(t)$ amplifies the prescribed displacement and illustrates the loading history according to equation $u(t) = p(t)u_o$.

In the numerical example we consider a cyclic loading program in tension with increasing mean value of the loading. The assumed loading program is illustrated in Fig. 2. For

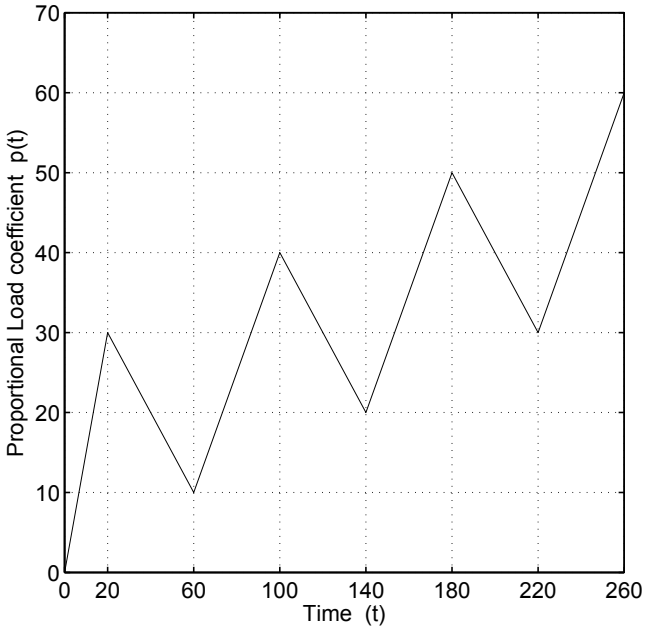

Figure 2: Cyclic loading program in tension with increasing mean value of the loading.

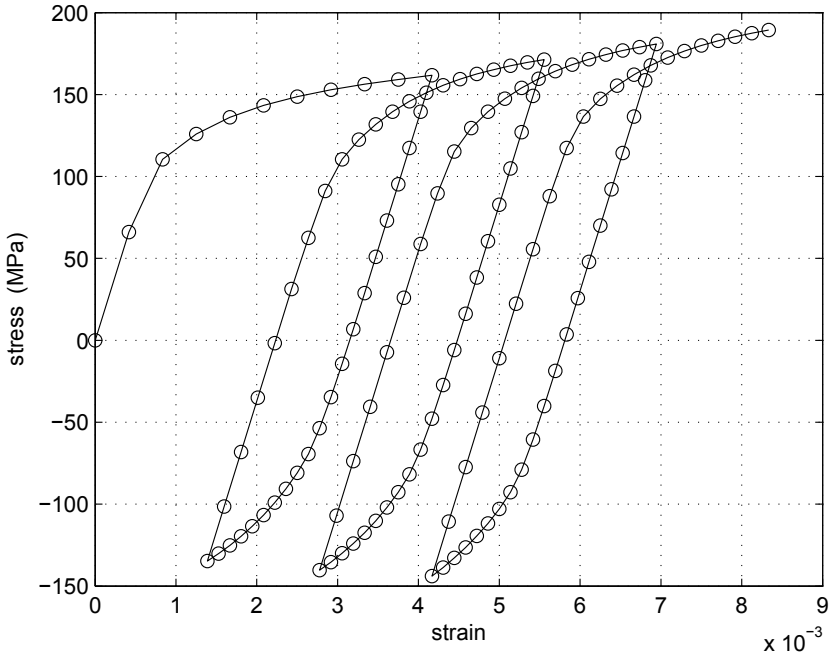

Figure 3: Average end stress versus average strain for the cyclic loading program given in Fig. 2. In the analysis a doubled time increment $\Delta t = 2$ has been adopted with $t_{max} = 260$.

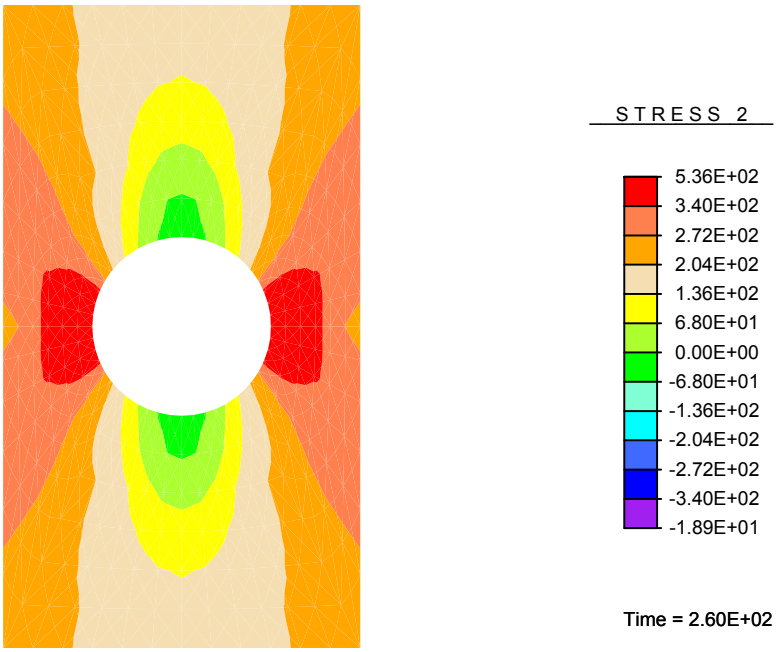

Figure 4: Contour plot of vertical stress in the strip for $t_{max} = 260$. Cyclic loading program in tension with loading program given in Fig. 2.

this loading program the average end stress versus the average strain is illustrated in Fig. 3. Herein the stress is averaged as the sum of the reactions on the boundary upper edge over the related area, the strain is averaged as the displacement at the boundary upper edge over the height. By exploiting symmetry properties, the final contour plot of the vertical stress in the strip is illustrated in Fig. 4 for $t_{max} = 260$.

The computational analysis of the Newton Raphson iterative procedure for the global structural problem shows a quadratic rate of asymptotic convergence. For more details on the convergence properties of the proposed algorithmic scheme, see De Angelis and Taylor [1] where a comprehensive treatment is presented.

7 CONCLUSIONS

In this work we presented an exact closed form solution of the return mapping algorithm in elastoplasticity with nonlinear kinematic hardening behavior, see also De Angelis and Taylor [1]. Nonlinear kinematic hardening rules have been adopted for modelling kinematic hardening behavior of ductile materials, see e.g. [2].

One of the advantages of the proposed formulation is to reduce the local constitutive equations of three-dimensional elastoplasticity problems to only one nonlinear scalar equation which ultimately condenses in a *quartic algebraic equation*. The formulation allows to find the analytical solution of the algebraic equation in exact closed form and, consequently, no iterative method is required to solve the local constitutive equations in three-dimensional elastoplasticity. The consistent tangent operator associated to the

proposed algorithmic scheme has been derived. The algorithmic formulation ensures a quadratic rate of asymptotic convergence for the global structural problem in elastoplasticity. The effectiveness of the proposed algorithmic scheme has been suitably illustrated by reporting numerical applications and computational results for complex and cyclic loading conditions.

REFERENCES

[1] De Angelis, F., and Taylor, R.L., "An efficient return mapping algorithm for elastoplasticity with exact closed form solution of the local constitutive problem", *Engineering Computations*, **32** (8), 2259 - 2291, (2015).

[2] Armstrong, P.J., and Frederick, C.O., "A mathematical representation of the multiaxial Bauschinger effect", Report RD/B/N731, CEGB, *Central Electricity Generating Board,* Berkeley, UK, (1966). Reprint in: Frederick, C.O., and Armstrong, P.J., "A mathematical representation of the multiaxial Bauschinger effect", *Mater. High Temp.*, **24** (1), 1-26, (2007).

[3] Zienkiewicz, O.C., Taylor, R.L., and Fox, D.D. *The Finite Element Method for Solid and Structural Mechanics*, 7th ed., Elsevier, Oxford, (2013).

[4] Simo, J.C., and Hughes, T.J.R., *Computational Inelasticity*, Springer-Verlag, Berlin, (1998).

[5] Prager, W., "Recent developments in the mathematical theory of plasticity", *J. Appl. Phys.*, **20**, (3), 235-241, (1949).

[6] Chaboche, J.L., "A review of some plasticity and viscoplasticity constitutive theories", *Int. J. Plasticity*, **24**, 1642-1693, (2008).

[7] Hartmann, S., Lührs, G., and Haupt, P., "An efficient stress algorithm with applications in viscoplasticity and plasticity", *Int. J. Num. Meth. Engrg.*, **40**, 991-1013, (1997).

[8] Kobayashi, M., and Ohno, N., "Implementation of cyclic plasticity models based on a general form of kinematic hardening", *Int. J. Num. Meth. Engrg.*, **53**, 2217-2238, (2002).

[9] De Angelis, F., Taylor, R.L., "A nonlinear finite element plasticity formulation without matrix inversions", *Finite Elements in Analysis and Design*, **112**, 11-25 , (2016).

[10] Auricchio, F., and Taylor, R.L., "Two material models for cyclic plasticity: nonlinear kinematic hardening and generalized plasticity", *Int. J. Plasticity*, **11**, 65-98, (1995).

[11] Abramowitz, M., "Solutions of quartic equations", in *Handbook of mathematical functions with formulas, graphs and mathematical tables*, M. Abramowitz and I.A. Stegun (Editors), 17-18, §3.8.3, Dover, New York, (1972).

[12] Beyer, W.H. *CRC Standard mathematical tables*, 28th ed., 12, CRC Press, Boca Raton, FL, (1987).

[13] Hacke, J.E. Jr., "A simple solution of the general quartic", *The American Mathematical Monthly*, **48**, (5), 327-328 , (1941).

[14] Nukala, P.K.V.V., "A return mapping algorithm for cyclic viscoplastic constitutive models" *Comput. Methods Appl. Mech. Engrg.*, **195**, 148-178, (2006).

[15] Artioli, E., Auricchio, F., and Beirao da Veiga, L., "Second-order accurate integration algorithms for the von-Mises plasticity with a nonlinear kinematic hardening mechanism" *Comput. Methods Appl. Mech. Engrg.*, **196**, 1827-1846, (2007).

[16] De Angelis, F., and Cancellara, D., "Multifield variational principles and computational aspects in rate plasticity", *Computers and Structures*, **180**, 27-39 , (2017).

[17] De Angelis, F., and Taylor, R.L., "Numerical algorithms for plasticity models with nonlinear kinematic hardening", in *11th World Congress on Computational Mechanics, WCCM XI, and 5th European Conference on Computational Mechanics, ECCM V*, Eds.: E. Onate, J. Oliver and A. Huerta, 20-25 july, 2014, EBook **VI**, 6560-6570, CIMNE, Barcellona, Spain, (2014).

[18] Artioli, E., Bisegna, P., "An incremental energy minimization state update algorithm for 3D phenomenological internal-variable SMA constitutive models based on isotropic flow potentials" *Int. J. Num. Meth. Engrg.*, **105** (3), 197-220, (2016).

[19] Artioli, E., Castellazzi, G., Krysl, P., "Assumed strain nodally integrated hexahedral finite element formulation for elastoplastic applications" *Int. J. Num. Meth. Engrg.*, **99** (11), 844-866, (2014).

[20] Castellazzi, G., Artioli, E., Krysl, P., "Linear tetrahedral element for problems of plastic deformation" *Meccanica*, **50** (12), 3069-3086, (2015).

[21] Taylor, R.L., "FEAP - A Finite Element Analysis Program, User Manual (Vers: 8.4)", `http://www.ce.berkeley.edu/feap`, (2017).